Rational design of an ESIPT-based fluorescent probe for selectively monitoring glutathione in live cells and zebrafish

Ya-Long Zheng, Han-Chen Zhang, Di-Hua Tian, De-Chen Duan, Fang Dai, Bo Zhou

PII: S1386-1425(20)30407-8

DOI: https://doi.org/10.1016/j.saa.2020.118429

Reference: SAA 118429

To appear in: *Spectrochimica Acta Part A: Molecular and Biomolecular Spectroscopy*

Received date: 15 February 2020

Revised date: 26 April 2020

Accepted date: 27 April 2020

Please cite this article as: Y.-L. Zheng, H.-C. Zhang, D.-H. Tian, et al., Rational design of an ESIPT-based fluorescent probe for selectively monitoring glutathione in live cells and zebrafish, *Spectrochimica Acta Part A: Molecular and Biomolecular Spectroscopy* (2020), https://doi.org/10.1016/j.saa.2020.118429

Rational design of an ESIPT-based fluorescent probe for selectively monitoring glutathione in live cells and zebrafish

Ya-Long Zheng, Han-Chen Zhang, Di-Hua Tian, De-Chen Duan, Fang Dai* and Bo Zhou*

State Key Laboratory of Applied Organic Chemistry, Lanzhou University, 222 Tianshui Street S., Lanzhou, Gansu 730000, China

———————————————————

*Corresponding author.

E-mail: bozhou@lzu.edu.cn; daifang@lzu.edu.cn

Abstract

Glutathione (GSH), an extremely important antioxidant, is a major participant in redox homeostasis and tightly associated with various clinical diseases. Thus, accurate and rapid detection of intracellular GSH is imperative to elucidate its role in physiological and pathological processes. Herein, by modifying 2-(2′-hydroxyphenyl) benzothiazole (HBT) scaffold, we developed an excited-state intramolecular proton transfer (ESIPT)-based fluorescent probe **BTFMD** for tracking glutathione, which exhibited good selectivity, excellent water solubility, a large Stokes shift (181 nm) and fast response rate (within 10 min). Furthermore, the probe was successfully applied for imaging of endogenous GSH in live cells and zebrafish, and probing into the role of GSH in the development of cancer and Parkinson's disease.

Keywords: Fluorescent probe; Glutathione; HBT; Excited-state intramolecular proton transfer; Parkinson's disease model; Zebrafish

1. Introduction

Glutathione (GSH), the most abundant intracellular biothiol, works as a cornerstone of maintaining redox homeostasis to avoid the oxidative damage of proteins, lipids and DNA induced by reactive oxygen species [1-4]. It is well-known that its abnormal levels are associated with various diseases, such as cardiovascular diseases, inflammation, cancers, Alzheimer's disease and Parkinson's disease [5-7]. Therefore, developing a specific method for detecting GSH is conducive to explore its role in pathophysiological processes.

Nowadays, the fluorescent detection method has attracted much attention for its irreplaceable role and significant advantages in life science [8-9], including non-destructive detection, excellent selectivity and high sensitivity [10-11]. A considerable number of fluorescent probes for sensing GSH have been developed based on different response mechanisms (see Table S1 and S2) [11], such as cleavage of sulfonate esters [12-14] or sulphonamide [15-17], cleavage of disulphide bonds followed by cyclization [18-20], Se-N bond cleavage [21-23], aryl substitution reactions [24-31], Michael additions and so on [32-38]. Among of them, the ones undergoing excited-state intramolecular proton transfer (ESIPT) are particularly attractive when compared to the classic fluorescence mechanisms (photoinduced electron transfer, intramolecular charge transfer and fluorescence resonance energy transfer), because of their uncommon large Stokes shifts and environmental sensitivity [39]. Moreover, most of ESIPT fluorophores can be utilized for ratiometric sensing due to its dual-emission spectra, which is particularly useful for quantitative detection

of target analytes [40-41]. However, because the ESIPT process is usually inhibited by the presence of polar and hydrogen bond donating solvents, lots of ESIPT-based fluorescent probes works with the assistant of some surfactants, such as cetyltrimethylammonium bromide (CTAB), which creates a sufficiently hydrophobic environment to produce or reinforce a fluorescence response [39]. The use of surfactants limits the biological application of ESIPT-based probes due to toxicity of surfactants at high concentrations. Furthermore, the performance of ESIPT-based GSH fluorescence probes still needs to be improved in terms of response time, selectivity, Stokes shift and water-solubility (Table S1). Especially developing those capable of effectively discriminating GSH from other biothiols including cysteine (Cys), homocysteine (Hcy) and cysteine-containing proteins remains a challenge, owing to their similar chemical properties.

Accordingly, inspired by previous works [42-43] we used 2-(2´-hydroxyphenyl) benzothiazole (HBT), a known ESIPT fluorophore [44], to design GSH selective probe 2-(benzo[*d*]thiazol-2-yl)-6-formyl-4-methylphenyl 2,4-dinitrobenzenesulfonate (**BTFMD**) (Scheme 1), where 2, 4-dinitrobenzenesulfonyl group functions as the trigger for its rapid cleavage to **BTFM-OH** by GSH, Cys and Hcy. To reduce the interference from Cys and Hcy, we incorporated an aldehyde moiety that could further cyclize with them, thereby quenching green fluorescence of **BTFM-OH** [45-46]. We envisioned that the combination of 2,4-dinitrobenzenesulfonyl group and aldehyde moiety enables this probe to distinguish GSH accurately and rapidly, without the need of introducing CTAB (Scheme 1).

Scheme 1 here

2. Experiment

2.1 Materials and instruments

All chemical reagents were purchased from Energy Chemical (Shanghai, China). RPMI-1640 medium, 6-OHDA, GSH, Cys, Hcy, BSA and NEM were obtained from Sigma-Aldrich (St. Louis, USA). Penicillin and streptomycin were purchased from Solarbio (Beijing, China). Fetal bovine serum (FBS) was a product from Rongye Biotechnology Co., Ltd (Lanzhou, China). Dulbecco's modified Eagle medium was purchased from Thermo Scientific. Zebrafish were obtained from Feixi Biotechnology Co., Ltd (Shanghai, China).

All reagents and solvents were commercially available and used without further purification unless otherwise stated. Deionized water was selected during all experiments. All reactions were magnetically stirred and monitored using thin layer chromatography. ^{1}H NMR and ^{13}C NMR spectra were measured by a Bruker AM - 400 MHz spectrometer. High-resolution mass spectra were collected on a High-Resolution Mass Spectrometer (HRMS, Bruker APEX Ⅱ 47e mass spectrometer). The UV/vis absorption spectra were obtained on a TU-1901 spectrophotometer. Fluorescence spectra were recorded on F-7000 FL spectrophotometer. The zebrafish imaging experiments were carried out using an Olympus IX71 inverted microscope.

*2.2 Synthesis of **BTFMD***

The probe **BTFMD** was readily synthesized by using simple and cheap raw materials. The details of the synthesis procedure and the characterization of compound were included in the Supporting Information.

BTFMD, white solid, mp: 213-215 ℃; ^{1}H NMR (400 MHz, $CDCl_3$, ppm): δ 10.44 (s, 1H), 8.23 (d, J = 2.0 Hz, 1H), 7.99 (d, J = 2.0 Hz, 1H), 7.87 (dd, J = 8.4, 2.0 Hz, 1H), 7.89-7.75 (m, 4H), 7.48-7.42 (m, 1H), 7.41-7.35 (m, 1H), 2.54 (s, 3H); ^{13}C NMR (100 MHz, $CDCl_3$, ppm): δ 186.9, 161.4, 152.6, 149.6, 146.0, 139.6, 137.4, 135.6, 133.7, 132.5, 132.0, 131.0, 128.4, 127.1, 126.6, 126.0, 123.4, 121.5, 119.6, 21.0; HRMS (ESI) Calcd. for $C_{20}H_{19}NO_4$ $(M+H)^+$: 500.0217, Found 500.0218.

2.3 Optical studies

The solutions of amino acids and reduced glutathione (GSH) were prepared in deionized water. The tested species included thiol compounds (GSH, Cys, Hcy), bovine serum albumin (BSA) and amino acids (His, Leu, Ile, Thr, Ala, Ser, Met, Lys, Pro, Val, Phe, Glu, Arg, Gly, Tyr, Trp, Asn, Asp and Gln). The stock solution of probe **BTFMD** was prepared in DMSO, and then diluted to 10 μM in 3 mL PBS buffer. Fluorescence spectra data were not recorded until 20 min after the addition of analytes. The excitation and emission slit width were 10 nm and 15 nm, respectively.

2.4 Cytotoxicity assays

HepG2 and PC12 cells were purchased from the Shanghai Institute of Biochemistry and Cell Biology, Chinese Academy of Sciences. In a humidified atmosphere 5% CO_2 at 37 °C, HepG2 cells and PC12 cells were cultured in RPMI medium 1640 and DMEM (Dulbecco's modified Eagle's medium) respectively, both of which supplemented with 10% fetal bovine serum (FBS), 100 U/mL penicillin, and 100 U/mL streptomycin. HepG2 cells (4×10^4 cells/well) and PC12 cells (6×10^4 cells/well) were seeded in 96 well plate for overnight, then pretreated with different concentrations of **BTFMD** and cultured for another 24 h. Subsequently, the cells were incubated with 10 μL methyl thiazolyl tetrazolium (MTT, 5 mg/mL) and 90 μL culture medium for 4 h, and absorbance of the solution at 570 nm was measured by using a Bio-Rad M680 microplate reader.

2.5 Cell fluorescence imaging

HepG2 cells (4×10^4 cells/well), HeLa cells (4×10^4 cells/well) and L02 cells (5×10^4 cells/well) were seeded in a 6-well culture plate for overnight and were incubated with probe **BTFMD**. Subsequently, the cells were washed three times with PBS (pH = 7.4) before fluorescence image. After cultured in a 6-well culture plate for overnight, PC12 cells (8×10^4 cells/well) were pretreated with different concentrations of 6-OHDA for 12 h and then incubated with **BTFMD** for 20 min. Fluorescence imaging was acquired by fluorescence microscope (Leica DM 4000B, United States).

2.6 Zebrafish imaging

For fluorescence imaging *in vivo*, 5-day-old zebrafish were divided into four groups and treated in different ways. Subsequently, they were washed with medium for three times and imaged with Olympus IX71 inverted microscope.

3. Result and discussion

3.1 Synthesis of probe

BTFMD was prepared by following the synthesis procedure shown in Scheme 2 [47-49]. Compound **1** was synthesized through cyclization of 5-methylsalicylaldehyde and 2-aminobenzenethiol, and then was used to react with hexamethylenetetramine to produce compound **2**. Finally, we obtained the probe **BTFMD** *via* the substitution reaction of compound **2** and 2, 4-dinitrobenzenesulfonyl chloride.

Scheme 2 here

3.2 Fluorescent response to GSH

Initially, the response of the probe to GSH was studied. As shown in Fig. 1A, the probe **BTFMD** in PBS buffer (pH = 7.4) exhibited a shoulder peak at about 372 nm after the addition of GSH. As expected, **BTFMD** displayed barely fluorescence, but manifested an enhancement of fluorescence at 553 nm upon the excitation at 372 nm when different concentrations of GSH were introduced (Fig. 1B), highlighting a large Stokes shift (181 nm). Furthermore, we explored the linear relationship between the fluorescence intensity and GSH concentrations (Fig. 1C), and calculated the detection limit (330 nM) of **BTFMD** based on the 3σ/k method. Time-dependent fluorescence

spectroscopy was introduced to check response rate of **BTFMD** to GSH in PBS. After addition of 1mM GSH, the fluorescence intensity gradually increased and reached equilibrium within 10 min (Fig. 1D), indicating that **BTFMD** could be a potential tool for rapid detection of GSH.

Figure 1 here

3.3 Studies on pH dependency and selectivity

Moreover, we evaluated the effect of different pH values on the fluorescent response of BTFMD to GSH. As shown in Figure 2A, the probe displayed a maximum response to GSH under physiological conditions (pH = 7), hinting at that it holds great promise for tracking GSH in living cells. To clarify the selectivity of **BTFMD** toward GSH, we benchmarked its performance on a variety of relevant species including biothiols (GSH, Cys and Hcy), bovine serum albumin (BSA, as the model of the cysteine-containing proteins) and various amino acids (His, Leu, Ile, Thr, Ala, Ser, Met, Lys, Pro, Val, Phe, Glu, Arg, Gly, Tyr, Trp, Asn, Asp and Gln). As illustrated in Fig. 2B, GSH induced a remarkable (34-fold) increase in the fluorescence intensity at 553 nm, followed by Cys, Hcy and BSA showing only a weak response, while various amino acids was inactive, highlighting the good selectivity of **BTFMD** toward GSH. These results suggest that the probe is suitable for selective imaging of glutathione in biological research.

Figure 2 here

3.4 Mechanistic investigation

To further verify our assumption, HRMS spectroscopy was used to explore the reaction mechanism. After the reaction of **BTFMD** with GSH, Cys and Hcy respectively, the key peaks of **BTFM-OH** (m/z = 270.06, $[M + H]^+$), **GSDN** (m/z = 474.09, $[M + H]^+$; m/z = 496.07, $[M + Na]^+$) and **BTMTA** (m/z = 373.07 and 387.08, $[M + H]^+$) were observed (Fig. S1-S3). In addition, when **BTFMD** was treated with Cys or Hcy (1mM), the fluorescence intensity increased firstly and then decreased at 553 nm which was accompanied by the gradual increment at 463 nm (Fig. S4-S5). These results are in line with our expectations (Scheme 1).

3.5 Fluorescent imaging

Prior to fluorescence imaging, the cytotoxicity of **BTFMD** was examined by the MTT assay from which 10 μM was found to be non-cytotoxic and thus used in the following experiments (Fig. S6). Next, the time-dependence of the fluorescence intensity of **BTFMD** toward endogenous GSH was investigated. When HepG2 cells were directly incubated with probe **BTFMD** for different time, the fluorescence intensity of green channel presented a time-dependent enhancement and reached a decent intensity at 20 min (Fig. 3A). In contrast, when the cells were pretreated with NEM (a thiol-trapping reagent), the fluorescence fainted over green channel (Fig. 3B). However, the NEM-pretreated cells were incubated with GSH, the fluorescence signal was observed again, implying that the probe could act as a sensitive detector of endogenous GSH.

Figure 3 here

Subsequently, with the aid of **BTFMD**, we evaluated the endogenous GSH levels of different cells (Fig. S7). It was found that the concentration of GSH in cancer cells (HepG2 and HeLa cells) was obviously higher than that in normal cells (L02 cells). The above result suggests that the probe is capable of effectively distinguishing cancer cells from normal cells in terms of GSH levels. This is also in tune with previous finding that compared with normal cells, cancer cells up-regulate GSH synthesis to cope with their inherent oxidative stress and maintain their malignant phenotype [50]. The abnormal GSH levels of cancer cells have opened a window for developing pro-oxidative anticancer agents to deplete their GSH [50-51]. We previously found a piperlongumine analog (PL-CL) that could induce more significantly the GSH depletion than its parent molecule (PL) [51]. This conclusion was verified again by using the probe (Fig. 4), supporting that it can help us screen pro-oxidative anticancer agents rapidly and facilitate pro-oxidative anti-cancer mechanistic investigation.

Figure 4 here

Parkinson's disease, a chronic progressive neurodegenerative disorder, is closely related to GSH level [52-53]. To explore the relationship, the PC12 cells treated with 6-hydroxydopamine (6-OHDA) were used to establish a cellular model of Parkinson's disease. Based on the cytotoxic results (Fig. S8), we adopted different concentrations

of 6-OHDA and **BTFMD** (5 μM) to carry out the following experiments. As shown in Fig. 5A and B, PC12 cells incubated with the probe displayed the dramatic green fluorescence. However, after PC12 cells were pretreated with 6-OHDA, the fluorescence intensity over green channel declined significantly (Fig. 5A and B) along with the death of partial cells (Fig. 5C), indicating that the pathophysiological processes of Parkinson's disease are closely associated with the GSH depletion.

Figure 5 here

Ultimately, to investigate the feasibility of **BTFMD** for monitoring GSH in vivo, we employed it to track GSH in living zebrafish. As shown in Fig. 6, zebrafish was directly incubated with the probe for 20 min and exhibited green fluorescence. In contrast, upon pretreatment with NEM, zebrafish exhibited faint green fluorescence. When the NEM-pretreated zebrafish was incubated with GSH, the green fluorescence signal appeared again. These results support that the probe holds promise for detecting endogenous GSH in living systems.

Figure 6 here

4. Conclusion

In summary, we designed a new GSH probe **BTFMD** by modifying the HBT scaffold based on the incorporation of the 2,4-dinitrobenzenesulfonyl group and aldehyde moiety. The probe is characterized by good selectivity, large Stokes shift, fast response rate, easy preparation and excellent water solubility, supporting that it is

suitable for tracking endogenous GSH. Subsequently, the probe was successfully applied to explore the role of GSH in the development of cancer and Parkinson's disease, as well as the activity and mechanism of pro-oxidative anticancer agents. Furthermore, the probe showed the satisfactory performance of fluorescence imaging in zebrafish. We anticipate that the probe would be a promising candidate to dissect the pathophysiological processes mediated by GSH.

Acknowledgements

This work was supported by the National Natural Science Foundation of China (Grant no. 21672091).

Conflict of interest

There are no conflicts of interest.

References

[1] I. S. Harris, A. E. Treloar, S. Inoue, M. Sasaki, C. Gorrini, K. C. Lee, K. Y. Yung, D. Brenner, C. B. Knobbe-Thomsen, M. A. Cox, A. Elia, T. Berger, D. W. Cescon, A. Adeoye, A. Brüstle, S. D. Molyneux, J. M. Mason, W. Y. Li, K. Yamamoto, A. Wakeham, H. K. Berman, R. Khokha, S. J. Done, T. J. Kavanagh, C.-W. Lam, T. W. Mak, Glutathione and Thioredoxin Antioxidant Pathways Synergize to Drive Cancer Initiation and Progression, Cancer Cell 27 (2015) 211-222.

[2] G. Noctor, C. H. Foyer, Ascorbate and glutathione: Keeping active oxygen under control, Annu. Rev. Plant Physiol. Plant Mol. Biol. 49 (1998) 249-279.

[3] F. Q. Schafer, G. R. Buettner, Redox environment of the cell as viewed through the redox state of the glutathione disulfide/glutathione couple, Free Radical. Biol. Med. 30 (2001) 1191-1212.

[4] G. Calabrese, B. Morgan, J. Riemer, Mitochondrial Glutathione: Regulation and Functions, . Antioxid. Redox Signal. 27 (2017) 1162-1177.

[5] W. M. Johnson, A. L. Wilson-Delfosse, J. J. Mieyal, Dysregulation of Glutathione Homeostasis in Neurodegenerative Diseases, Nutrients 4 (2012) 1399-1440.

[6] D. M. Townsend, K. D. Tew, H. Tapiero, The importance of glutathione in human disease, Biomed. Pharmacother. 57 (2003) 145-155.

[7] R. Dringen, Metabolism and functions of glutathione in brain, Prog. Neurobiol. 62 (2000) 649-671.

[8] Y. K. Yue, F. J. Huo, F. Q. Cheng, X. J. Zhu, T. Mafireyi, R. M. Strongin, C. X. Yin, Functional synthetic probes for selective targeting and multi-analyte detection

and imaging, Chem. Soc. Rev. 48 (2019) 4155-4177.

[9] P. Gao, W. Pan, N. Li, B. Tang, Fluorescent probes for organelle-targeted bioactive species imaging, Chem. Sci. 10 (2019) 6035-6071.

[10] C. X. Yin, K. M. Xiong, F. J. Huo, J. C. Salamanca, R. M. Strongin, Fluorescent Probes with Multiple Binding Sites for the Discrimination of Cys, Hcy, and GSH, Angew. Chem. Int. Ed. 56(2017) 13188-13198.

[11] S. Lee, J. Li, X. Zhou, J. Yin, J. Yoon, Recent progress on the development of glutathione (GSH) selective fluorescent and colorimetric probes, Coord. Chem. Rev. 366 (2018) 29-68, (and references therein).

[12] W. Jiang, H. Chen, Y. Pan, W. Lin, A long-wavelength fluorescent turn-on probe for video detection of biological thiols in living cells, Anal. Methods. 7 (2015) 4168-4172.

[13] X. Dai, T. Zhang, J.-Y. Miao and B.-X. Zhao, A ratiometric fluorescent probe with DNBS group for biothiols in aqueous solution, Sens. Actuatorsn B: Chem. 223 (2016) 274-279.

[14] C. Wang, Y. Wang, G. Wang, S. Chen, C. Huang, Two-isophorone fluorophore-based design of a ratiometric fluorescent probe and its application in the sensing of biothiols, J. Mater. Chem. B 7 (2019) 5633-5639.

[15] J. Yin, Y. Kwon, D. Kim, D. Lee, G. Kim, Y. Hu, J.-H. Ryu, J. Yoon, Cyanine-Based Fluorescent Probe for Highly Selective Detection of Glutathione in Cell Cultures and Live Mouse Tissues, J. Am. Chem. Soc. 136 (2014) 5351-5358.

[16] G.-J. Kim, D.-H. Yoon, M.-Y. Yun, H. Kwon, H.-J. Ha, H.-J. Kim, An activatable fluorescent probe for targeting cellular membrane through the biothiol-mediated hydrazone-to-pyrazole transformation, Sens. Actuatorsn B: Chem. 211 (2015) 245-249.

[17] H. Zhang, C. Wang, G. Wang, K. Wang, K. Jiang, Thrombin-mediated ratiometric two-photon fluorescent probe for selective imaging of endogenous ultratrace glutathione in platelet, Biosens. Bioelectron. 78 (2016) 344-350.

[18] B. C. Zhu, X. L. Zhang, Y. M. Li, P. F. Wang, H. Y. Zhang, X. Q. Zhuang, A colorimetric and ratiometric fluorescent probe for thiols and its bioimaging applications, Chem. Commun. 46 (2010) 5710-5712.

[19] M. H. Lee, J. H. Han, P.-S. Kwon, S. Bhuniya, J. Y. Kim, J. L. Sessler, C. Kang, J. S. Kim, Hepatocyte-Targeting Single Galactose-Appended Naphthalimide: A Tool for Intracellular Thiol Imaging in Vivo, J. Am. Chem. Soc. 134 (2012) 1316-1322.

[20] C. S. Lim, G. Masanta, H. J. Kim, J. H. Han, H. M. Kim, B. R. Cho, Ratiometric Detection of Mitochondrial Thiols with a Two-Photon Fluorescent Probe, J. Am. Chem. Soc. 133 (2011) 11132-11135.

[21] B. Tang, Y. Xing, P. Li, N. Zhang, F. Yu, G. Yang, A Rhodamine-Based Fluorescent Probe Containing a Se−N Bond for Detecting Thiols and Its Application in Living Cells, J. Am. Chem. Soc. 129 (2007) 11666-11667.

[22] X. Zeng, X. Zhang, B. Zhu, H. Jia, W. Yang, Y. Li, J. Xue, A colorimetric and ratiometric fluorescent probe for quantitative detection of GSH at physiologically

relevant levels, Sens. Actuators B: Chem. 159 (2011) 142-147.

[23] K. Xu, M. Qiang, W. Gao, R. Su, N. Li, Y. Gao, Y. Xie, F. Kong, B. Tang, A near-infrared reversible fluorescent probe for real-time imaging of redox status changes in vivo, Chem. Sci. 4 (2013) 1079-1086.

[24] L.-Y. Niu, Y.-S. Guan, Y.-Z. Chen, L.-Z. Wu, C.-H. Tung, Q.-Z. Yang, BODIPY-Based Ratiometric Fluorescent Sensor for Highly Selective Detection of Glutathione over Cysteine and Homocysteine , J. Am. Chem. Soc. 134 (2012) 18928-18931.

[25] S.-Y. Lim, K.-H. Hong, D.I. Kim, H. Kwon, H.-J. Kim, Tunable Heptamethine–Azo Dye Conjugate as an NIR Fluorescent Probe for the Selective Detection of Mitochondrial Glutathione over Cysteine and Homocysteine, J. Am. Chem. Soc. 136 (2014) 7018-7025.

[26] J. Liu, Y.-Q. Sun, H. Zhang, Y. Huo, Y. Shi, W. Guo, Simultaneous fluorescent imaging of Cys/Hcy and GSH from different emission channels, Chem. Sci. 5 (2014) 3183-3188.

[27] Y.-Q. Sun, J. Liu, H. Zhang, Y. Huo, X. Lv, Y. Shi, W. Guo, A Mitochondria-Targetable Fluorescent Probe for Dual-Channel NO Imaging Assisted by Intracellular Cysteine and Glutathione, J. Am. Chem. Soc. 136 (2014) 12520-12523.

[28] F. Wang, L. Zhou, C. Zhao, R. Wang, Q. Fei, S. Luo, Z. Guo, H. Tian, W.-H. Zhu, A dual-response BODIPY-based fluorescent probe for the discrimination of glutathione from cystein and homocysteine, Chem. Sci. 6 (2015) 2584-2589.

[29] C. Xu, H. Li, B. Yin, A colorimetric and ratiometric fluorescent probe for selective detection and cellular imaging of glutathione, Biosens. Bioelectron. 72 (2015) 275-281.

[30] Y. Kim, S.V. Mulay, M. Choi, S.B. Yu, S. Jon, D.G. Churchill, Exceptional time response, stability and selectivity in doubly-activated phenyl selenium-based glutathione-selective platform, Chem. Sci. 6 (2015) 5435-5439.

[31] X. Xie, M. Li, F. Tang, Y. Li, L. Zhang, X. Jiao, X. Wang, B. Tang, Combinatorial Strategy to Identify Fluorescent Probes for Biothiol and Thiophenol Based on Diversified Pyrimidine Moieties and Their Biological Applications, Anal. Chem. 89 (2017) 3015-3020.

[32] X. Chen, S.-K. Ko, M. J. Kim, I. Shin, J. Yoon, A thiol-specific fluorescent probe and its application for bioimaging, Chem. Commun. 46 (2010) 2751-2753.

[33] K. Umezawa, M. Yoshida, M. Kamiya, T. Yamasoba, Y. Urano, Rational design of reversible fluorescent probes for live-cell imaging and quantification of fast glutathione dynamics, Nat. Chem. 9 (2017) 279-286.

[34] G. Yin, T. Niu, T. Yu, Y. Gan, X. Sun, P. Yin, H. Chen, Y. Zhang, H. Li and S. Yao, Simultaneous Visualization of Endogenous Homocysteine, Cysteine, Glutathione, and their Transformation through Different Fluorescence Channels, Angew. Chem. Int. Ed. 58 (2019) 4557-4561.

[35] Z. Xu, X. Huang, X. Han, D. Wu, B. Zhang, Y. tan, M. Cao, S. H. Liu, J. Yin, J. Yoon, A visible and near-infrared, dual-channel fluorescence-on probe for selectively tracking mitochondrial glutathione, Chem 4 (2018) 1609-1628.

[36] H. Zhang, L. Xu, W. Chen, J. Huang, C. Huang, J. Sheng, X. Song, Simultaneous Discrimination of Cysteine, Homocysteine, Glutathione, and H2S in Living Cells through a Multisignal Combination Strategy, Anal. Chem. 91 (2019) 1904-1911.

[37] J. Chen, X. Jiang, S.L. Carroll, J. Huang, J. Wang, Theoretical and Experimental Investigation of Thermodynamics and Kinetics of Thiol-Michael Addition Reactions: A Case Study of Reversible Fluorescent Probes for Glutathione Imaging in Single Cells, Org. Lett. 17 (2015) 5978-5981.

[38] L. He, Q. Xu, Y. Liu, H. Wei, Y. Tang, W. Lin, Coumarin-Based Turn-On Fluorescence Probe for Specific Detection of Glutathione over Cysteine and Homocysteine, ACS Appl. Mater. Interfaces 7 (2015) 12809-12813.

[39] A. C. Sedgwick, L. Wu, H.-H. Han, S. D. Bull, X.-P. He, T. D. James, J. L. Sessler, B. Z. Tang, H. Tian, J. Yoon, Excited-state intramolecular proton-transfer (ESIPT) based fluorescence sensors and imaging agents, Chem. Soc. Rev. 47 (2018) 8842-8880.

[40] Y. Wang, H. Xiang, R. Zhao, C. Huang, A renewable test strip combined with solid-state ratiometric fluorescence emission spectra for the highly selective and fast determination of hydrazine gas, Analyst 143 (2018) 3900-3906.

[41] L. Wu, Y. Wang, M. Weber, L. Liu, A. C. Sedgwick, S. D. Bull, C. Huang, T. D. James, ESIPT-based ratiometric fluorescence probe for the intracellular imaging of peroxynitrite, Chem. Commun. 54 (2018) 9953-9956.

[42] Z. Huang, S. Ding, D. Yu, F. Huang, G. Feng, Aldehyde group assisted thiolysis of dinitrophenyl ether: a new promising approach for efficient hydrogen sulfide

probes, Chem. Commun. 50 (2014) 9185-9187.

[43] S. Chen, H. M. Li, P. Hou, A novel cyanobiphenyl benzothiazole-based fluorescent probe for detection of biothiols with a large Stokes shift and its application in cell imaging, Tetrahedron 73 (2017) 589-593.

[44] P. F. Barbara, L. E. Brus, P. M. Rentzepis, Intramolecular proton transfer and excited-state relaxation in 2-(2-hydroxyphenyl)benzothiazole, J. Am. Chem. Soc. 102 (1980) 5631-5635.

[45] Y. Wang, L. J. Wang, E. K. Jiang, M. Q. Zhu, Z. Wang, S. S. Fan, Q. Gao, S. Z. Liu, Q. X. Li, R. M. Hua, A colorimetric and ratiometric dual-site fluorescent probe with 2,4-dinitrobenzenesulfonyl and aldehyde groups for imaging of aminothiols in living cells and zebrafish, Dyes Pigments 156 (2018) 338-347.

[46] L. Tang, J. Shi, Z. Huang, X. Yan, Q. Zhang, K. Zhong, S. Hou, Y. Bian, An ESIPT-based fluorescent probe for selective detection of homocysteine and its application in live-cell imaging, Tetrahedron Lett. 57 (2016) 5227-5231.

[47] H. Wen, Q. Huang, X. F. Yang, H. Li, Spirolactamized benzothiazole-substituted N,N-diethylrhodol: a new platform to construct ratiometric fluorescent probes, Chem. Commun. 49 (2013) 4956-4958.

[48] D. Dahal, L. McDonald, X. Bi, C. Abeywickrama, F. Gombedza, M. Konopka, S. Paruchuri, Y. Pang, An NIR-emitting lysosome-targeting probe with large Stokes shift via coupling cyanine and excited-state intramolecular proton transfer, Chem. Commun. 53 (2017) 3697-3700.

[49] L. Zeng, S. Chen, T. Xia, C. Zhong, Z. Liu, Designing two-photon fluorescent

probes based on the target-induced enhancement of the absorption cross-section, Chem. Commun. 50 (2014) 11139-11142.

[50] D. Trachootham, J. Alexandre, P. Huang, Targeting cancer cells by ROS-mediated mechanisms: a radical therapeutic approach?, Nat. Rev. Drug Discov. 8 (2009) 579-591.

[51] W.-J. Yan, Q. Wang, C.-H. Yuan, F. Wang, Y. Ji, F. Dai, X.-L. Jin, B. Zhou, Designing piperlongumine-directed anticancer agents by an electrophilicity-based prooxidant strategy: a mechanistic investigation, Free Radic. Biol. Med. 97 (2016) 109-123.

[52] L. V. Kalia, A. E. Lang, Parkinson's disease, Lancet 386 (2015), 896-912.

[53] D. A. Di Monte, P. Chan, M. S. Sandy, Glutathione in Parkinson's disease: a link between oxidative stress and mitochondrial damage? Ann Neurol. 32 (1992) S111-S115.

Figure legends

Scheme 1. Design of fluorescent probe **BTFMD** for selective tracking GSH.

Scheme 2. Synthesis of **BTFMD**

Figure 1. (A) Absorption spectra of **BTFMD** (10 μM) with and without GSH (1 mM) in PBS buffer (pH = 7.4). (B) Fluorescence response of **BTFMD** (10 μM) upon addition of GSH (0-1 mM) for 20 min in PBS (λ_{ex} = 372 nm). (C) The linear relationship of fluorescence intensity at 553 nm against the concentrations of GSH (0-15 μM). Incubation time: 20 min. (D) Time-dependent fluorescence spectra of **BTFMD** (10 μM) in the presence of 1 mM GSH at λ_{em} = 553 nm.

Figure 2. (A) Fluorescence intensity of probe **BTFMD** (10 μM) with 1 mM GSH in PBS with different pH conditions at 553 nm. Incubation time: 20 min. (B) Fluorescence response of **BTFMD** (10 μM) at λ_{em} = 553 nm, in the presence of biothiols (Cys, 1 mM; Hcy, 1 mM; GSH, 1 mM), BSA (100 μM) and various amino acids (100 μM) after incubating for 20 min in PBS (pH = 7.4).

Figure 3. (A) Fluorescence images of probe **BTFMD** (10 μM) in HepG2 cells under different time. Scale bar: 20 μm. (B) (b, f) HepG2 cells were incubated with BTFMD (10 μM) for 20min. (c, g) HepG2 cells were pretreated with NEM (1 mM) for 30 min and incubated with **BTFMD** (10 μM) for 20 min. (d, h) HepG2 cells were treated with

NEM (1 mM) for 30 min, GSH (1 mM) for 30 min, and then incubated with **BTFMD** (10 μM) for 20min. Scale bar: 20 μm.

Figure 4. (A) Fluorescence images of GSH in HepG2 cells pretreated with 5 μM PL or 5 μM PL-CL for 12 h followed by incubation with **BTFMD** (10 μM) for 20 min. (B) Relative fluorescence intensities in panel A. Scale bar: 50 μm.

Figure 5. Practical application of **BTFMD**. (A) PC12 cells pretreated with different concentrations of 6-OHDA for 12 h, and then incubated with **BTFMD** (5 μM) for 20 min. Scale bar: 50 μm. (B) Relative fluorescence intensities in panel A. (C) MTT assay of PC12 cells with different concentrations of 6-OHDA in 12 h and 24 h.

Figure 6. Fluorescence images of exogenous GSH in 5-day-old zebrafish. (b, f) Zebrafish was incubated with **BTFMD** (10 μM) for 15 min. (c, g) Zebrafish was pretreated with NEM (100 μM) for 20 min and incubated with **BTFMD** (10 μM) for 15 min. (d, h) Zebrafish was treated with NEM (100 μM) for 20 min, GSH (200 μM) for 20 min, and then incubated with **BTFMD** (10 μM) for 15 min. Scale bar: 200 μm.

Fang Dai and Bo Zhou designed the research, supervised the whole project and wrote the manuscript which was reviewed by all the authors; Ya-Long Zheng performed research. Han-Chen Zhang, Di-Hua Tian, and De-Chen Duan contributed to data analysis, with input from Fang Dai and Bo Zhou. All authors have read and approved this version of the article.

Declaration of interests

☒ The authors declare that they have no known competing financial interests or personal relationships that could have appeared to influence the work reported in this paper.

☐The authors declare the following financial interests/personal relationships which may be considered as potential competing interests:

Graphical abstract

Highlights

- ✓ **BTFMD** is readily synthesized with using simple and cheap raw materials.
- ✓ **BTFMD** is an ESIPT-based fluorescent probe for rapidly distinguish GSH.
- ✓ **BTFMD** has good selectivity, large Stokes shift and fast response rate.
- ✓ **BTFMD** has been successfully applied for imaging of endogenous GSH.

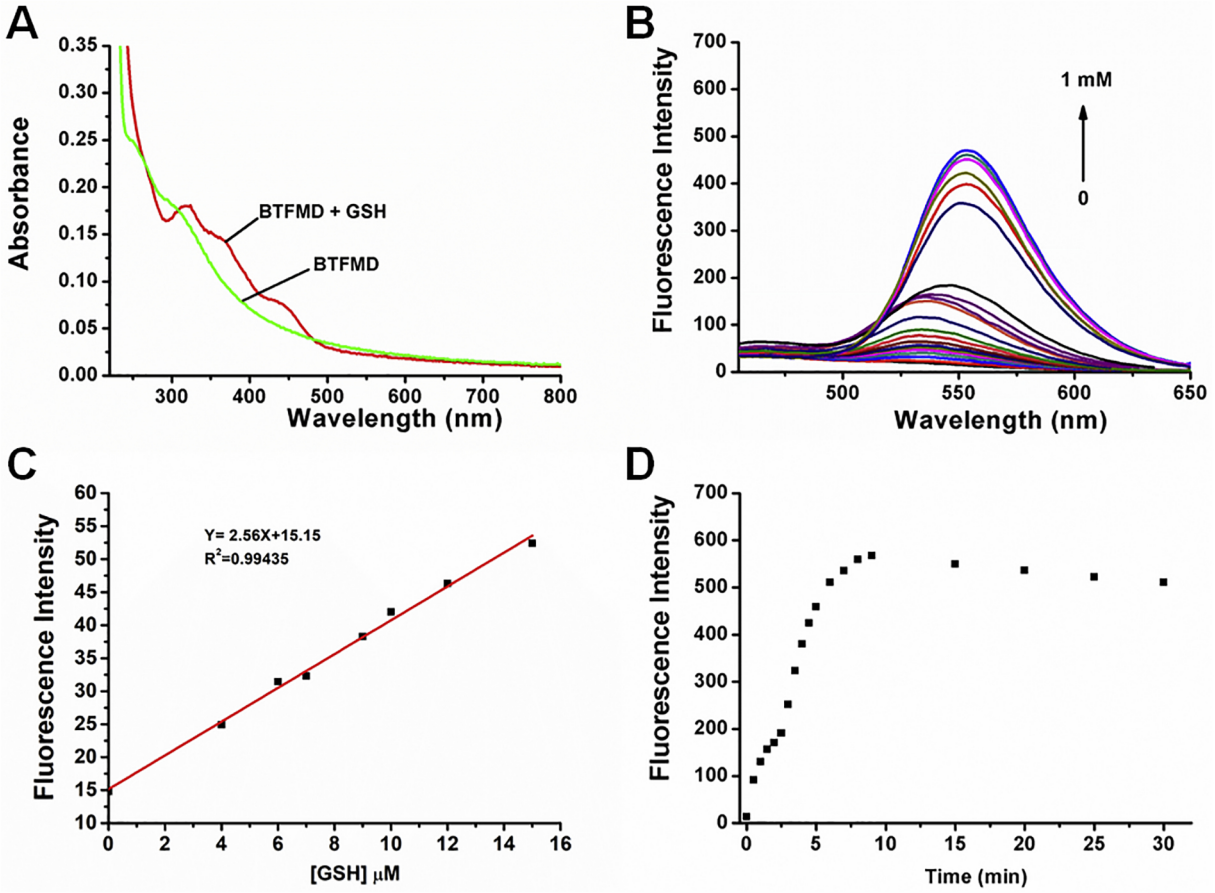
A
Absorbance
Wavelength (nm)
BTFMD + GSH
BTFMD
B
Fluorescence Intensity
Wavelength (nm)
1 mM
0
C
Fluorescence Intensity
[GSH] μM
Y= 2.56X+15.15
R²=0.99435
D
Fluorescence Intensity
Time (min)

Figure 1

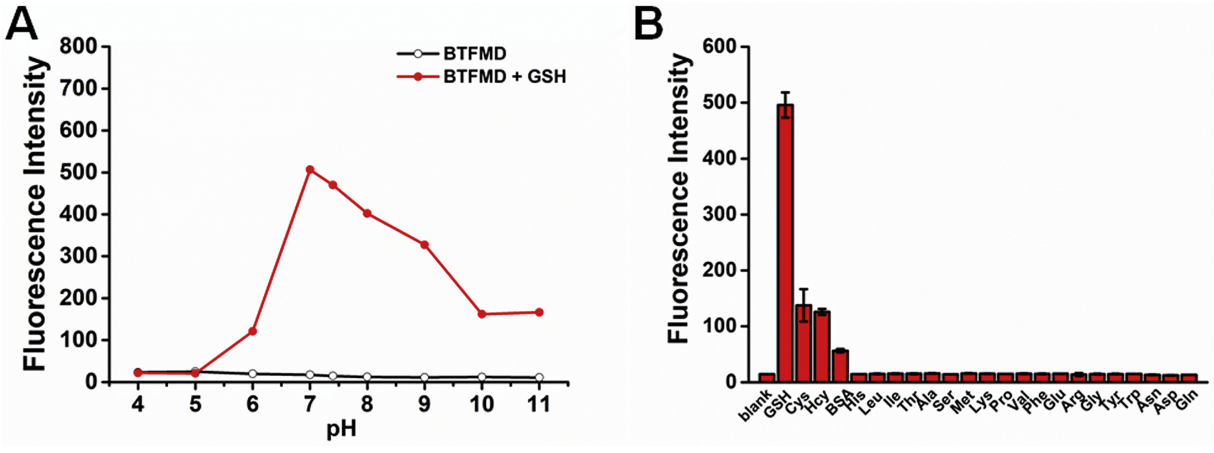
A
Fluorescence Intensity
800
700
600
500
400
300
200
100
0
4
5
6
7
8
9
10
11
pH
BTFMD
BTFMD + GSH
B
Fluorescence Intensity
600
500
400
300
200
100
0
blank
GSH
Cys
Hcy
BSA
His
Leu
Ile
Thr
Ala
Ser
Met
Lys
Pro
Val
Phe
Glu
Arg
Gly
Tyr
Trp
Asn
Asp
Gln

Figure 2

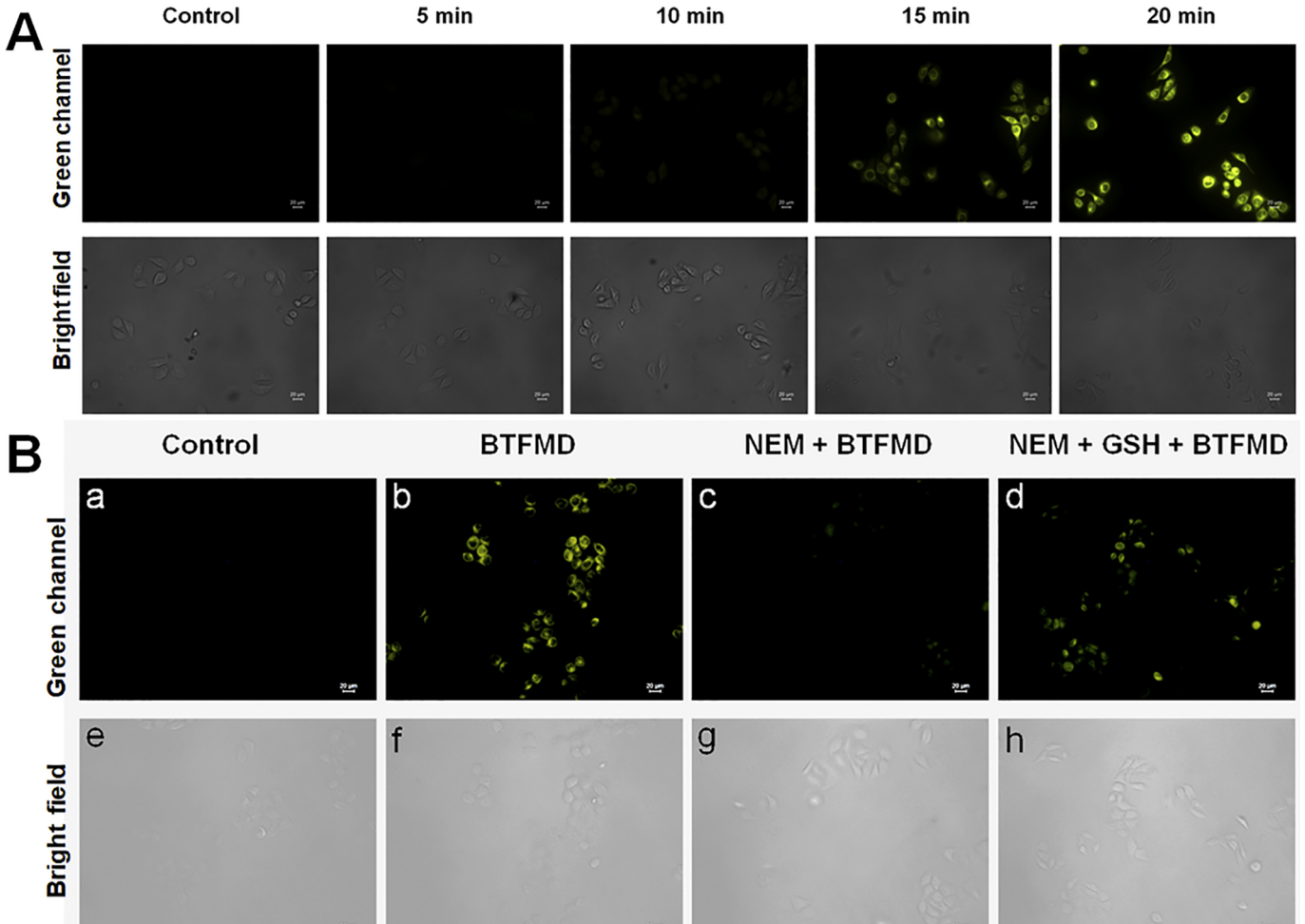
A
Control
5 min
10 min
15 min
20 min
Green channel
Bright field
B
Control
BTFMD
NEM + BTFMD
NEM + GSH + BTFMD
Green channel
Bright field
a
b
c
d
e
f
g
h

Figure 3

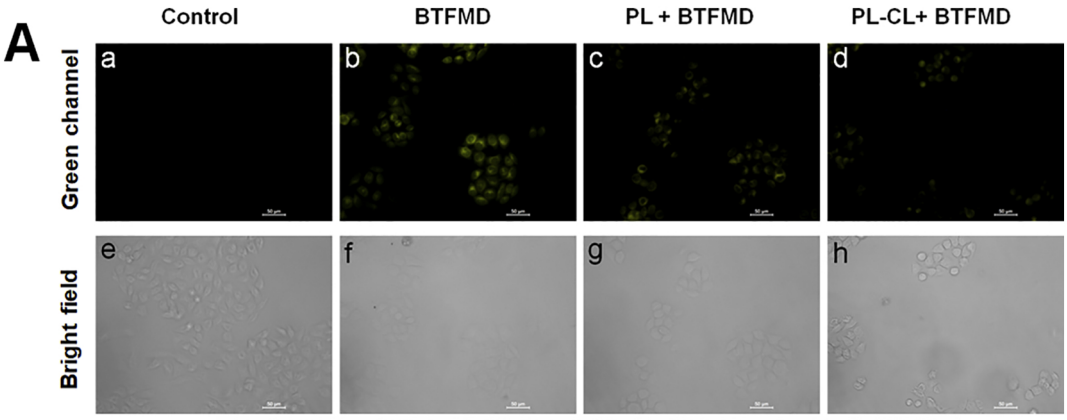
A
Control
BTFMD
PL + BTFMD
PL-CL+ BTFMD
Green channel
Bright field
a
b
c
d
e
f
g
h

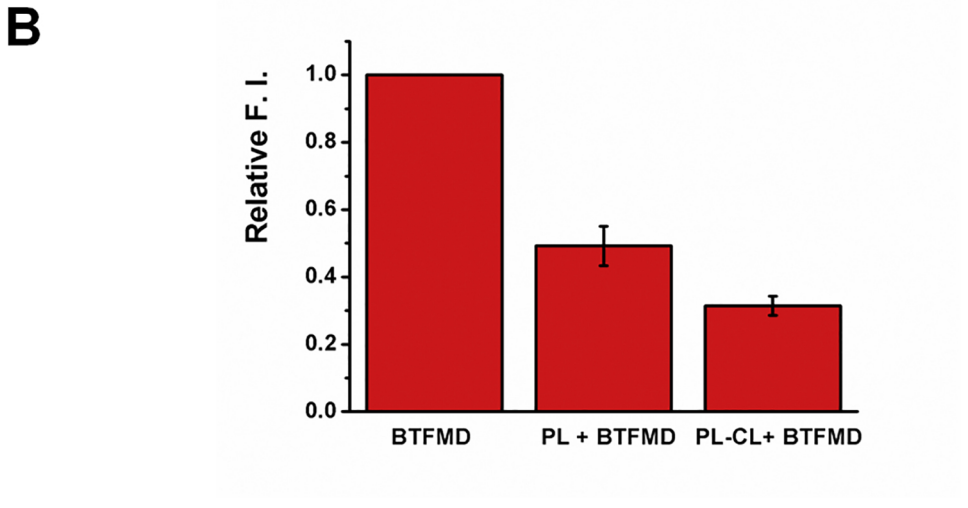
B
Relative F. I.
1.0
0.8
0.6
0.4
0.2
0.0
BTFMD
PL + BTFMD
PL-CL+ BTFMD

Figure 4

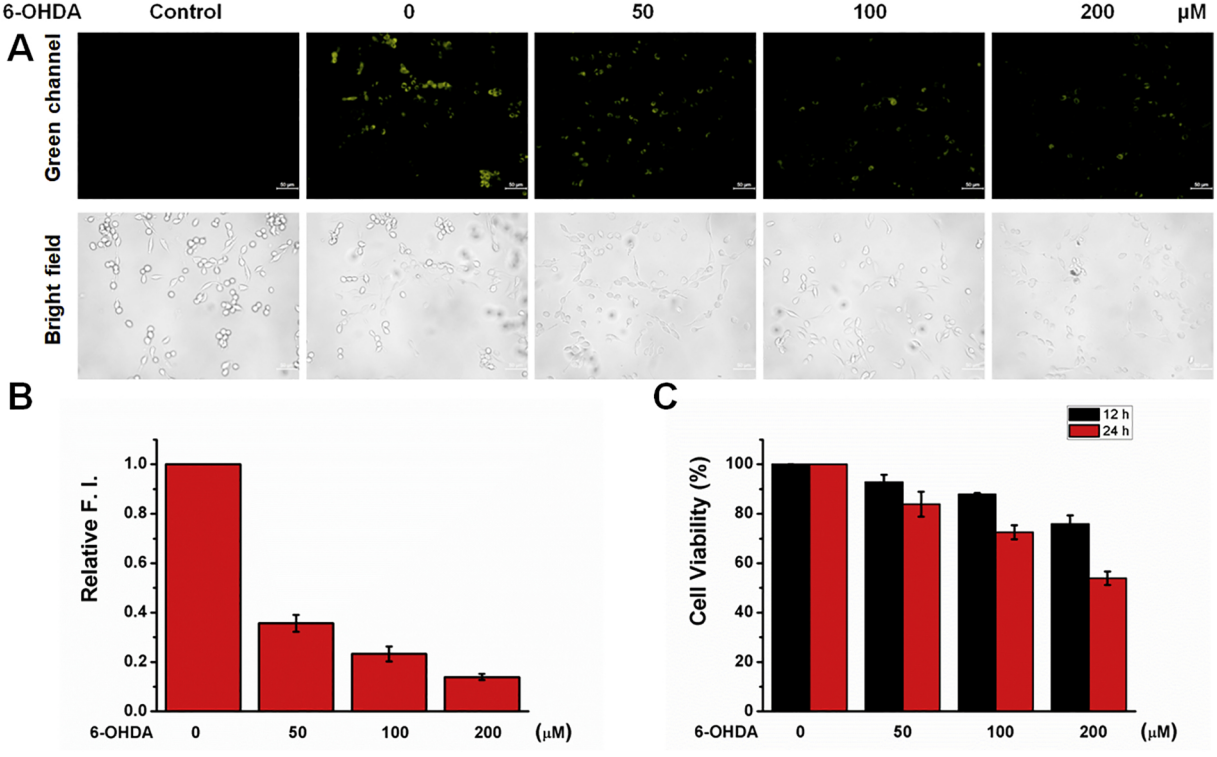
6-OHDA
Control
0
50
100
200
μM
A
Green channel
Bright field
B
Relative F. I.
1.0
0.8
0.6
0.4
0.2
0.0
6-OHDA
0
50
100
200
(μM)
C
12 h
24 h
Cell Viability (%)
100
80
60
40
20
0
6-OHDA
0
50
100
200
(μM)

Figure 5

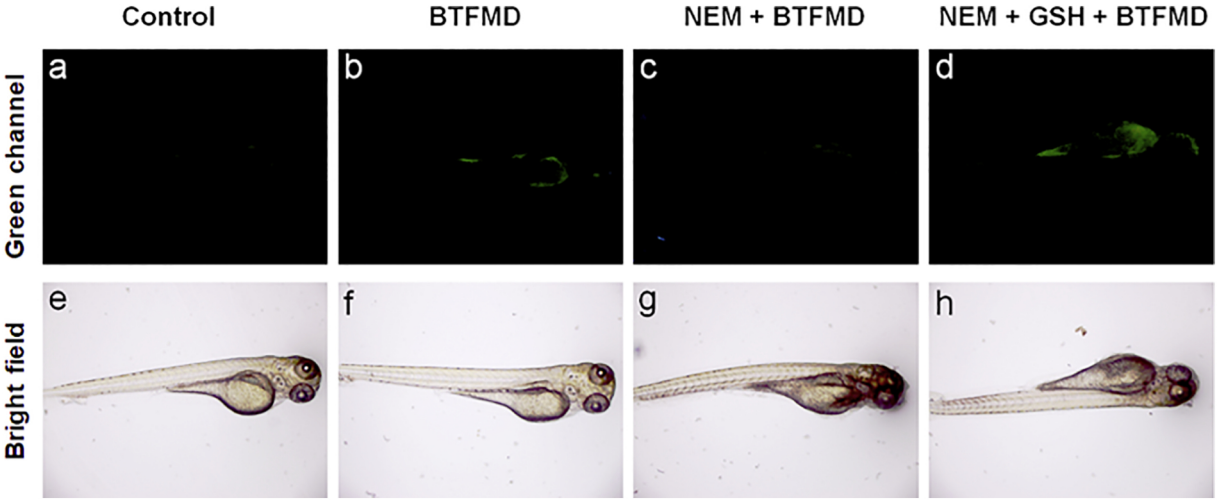
Control
BTFMD
NEM + BTFMD
NEM + GSH + BTFMD
Green channel
Bright field
a
b
c
d
e
f
g
h

Figure 6